



Isolation of a feline-derived feline panleukopenia virus with an A300P substitution in the VP2 protein and confirmation of its pathogenicity in dogs

Jiakang Li^{1,2†}, Jijia Peng^{3†}, Yue Zeng³, Ying Wang³, Luying Li^{1,2}, Yiran Cao⁴, Longlong Cao^{1,2}, QingXiu Chen³, Zijun Ye^{1,2}, Dengyuan Zhou^{1,2,3}, Shengbo Cao^{1,2*} and Qiuyan Li^{1,2*}

Abstract

Feline panleukopenia virus (FPV) is a single-stranded DNA virus that can infect cats and cause feline panleukopenia, which is a highly contagious and fatal disease in felines. The sequence of FPV is highly variable, and mutations in the amino acids of its capsid protein play crucial roles in altering viral virulence, immunogenicity, host selection, and other abilities. In this study, the epidemiology of FPV was studied using 746 gastrointestinal swab samples derived from cats that presented gastrointestinal symptoms specifically, diarrhea or vomiting during the period spanning from 2018 to 2022. The overall prevalence of FPV-positive patients among these samples was determined to be 45.4%. Capsid (virion) protein 2 (VP2) gene of each FPV-positive sample was sequenced and amplified, yielding 65 VP2 sequences. Among them, six VP2 gene sequences were detected in the majority of the samples test positive for FPV, and these positive samples originated from a diverse range of geographical locations. These isolates were named FPV-6, FPV-10, FPV-15, FPV-251, FPV-271 and FPV-S2. Additionally, the substitution of Ala300Pro (A300P) in VP2 was detected for the first time in feline-derived FPV (FPV-251). FPV-251 isolate, with this substitution in VP2 protein, exhibited stable proliferative capacity in Madin-Darby canine kidney (MDCK) cells and A72 cells. FPV-271 was selected as the FPV control isolate due to its single amino acid difference from VP2 protein of FPV-251 at position 300 (FPV-271 has alanine, while FPV-251 has proline). After oral infection, both FPV-251 and FPV-271 isolates caused feline panleukopenia, which is characterized by clinical signs of enterocolitis. However, FPV-251 can infect dogs through the oral route and cause gastrointestinal (GI) symptoms with lesions in the intestine and mesenteric lymph nodes (MLNs) of infected dogs. This is the first report on the presence of an A300P substitution in VP2 protein of feline-derived FPV. Additionally, FPV isolate with a substitution of A300P at VP2 protein demonstrated efficient replication capabilities in canine cell lines and the ability to infect dogs.

Keywords Feline panleukopenia virus, FPV, Dogs, VP2 gene characteristic, Host range

[†]Jiakang Li and Jijia Peng contributed equally to this work.

*Correspondence:

Shengbo Cao

sbcao@mail.hzau.edu.cn

Qiuyan Li

lqylqy6@webmail.hzau.edu.cn

Full list of author information is available at the end of the article

Introduction

Carnivore protoparvovirus 1 is a viral species of the *Protoparvovirus* genus in the *Parvoviridae* family (Cotmore et al. 2019). Parvoviruses are small, nonenveloped, linear single-stranded DNA viruses that infect invertebrates and vertebrates, making them evolutionarily successful species of viruses (Yuan et al. 2020). In recent years,



there has been a dramatic increase in pet ownership and cat breeding, leading to an increase in infectious diseases caused by viruses. Notably, feline calicivirus (FCV), feline leukemia virus (FeLV), and feline panleukopenia virus (FPV) are the most common infectious agents (Cao et al. 2022; Capozza et al. 2021; Xue et al. 2023). FPV is a widespread contagious virus in the Parvoviridae family, and it poses a significant threat to the safety of felines, particularly cats (Chowdhury et al. 2021). FPV infections typically result in leukopenia, fever, vomiting, and diarrhea. A mortality rate of 70% to 80% in kittens was reported in previous studies (Barrs 2019; Langeveld et al. 1993). After infection, FPV primarily proliferates in feline intestines, thus resulting in inflammation of the digestive tract. Acutely infected cats die within three days, and surviving cats gradually alleviate symptoms but are continuously detoxified through fecal matter and vomiting. Several FPV vaccines have been distributed globally, with products such as NOBIVAC® FELINE 1-HCP and Fel-O-Vax® PCT commanding significant market shares and enjoying widespread market acceptance. Nevertheless, only Fel-O-Vax is approved for use in China, utilizing CU-4 strain of FPV vaccine (Parrish 1991). Consequently, given the prevailing circumstances regarding pet cat vaccines in China, numerous Chinese facilities have initiated the development and manufacture of FPV vaccines, aiming to expedite the prevention and control of feline diseases in domestic cats.

FPV was initially discovered by Verge J in 1928 (Battilani et al. 2006). The FPV genome is composed of single-stranded DNA and contains two major open reading frames (ORFs) encoding two structural proteins, VP1 and VP2, and two nonstructural proteins, NS1 and NS2 (Cotmore and Tattersall 1987). The VP2 protein comprises more than 90% of the FPV capsid and acts as a receptor-binding protein. It plays a pivotal role in crucial stages of viral infection, specifically through its binding to the transferrin receptor (Hueffer et al. 2003). As a result, it exerts substantial influence on viral invasion, the regulation of virulence, and diverse associated processes. Notably, amino acid mutations at specific sites in VP2 can alter virus characteristics, thereby impacting pathogenesis and host range. This host range alteration in FPV may be a result of changes in the amino acid residues at sites 80, 93, 323, 564 or 568 of the VP2 protein (Truyen et al. 1995). In recent years, changes in amino acid residues at other sites in the VP2 protein have been reported to also affect the host range of FPV. For example, the unique substitution Gly(G)299Glu(E) in the capsid protein VP2 of the Giant panda/CD/2018 strain is considered to be related to the ability of FPV to infect pandas (Yi et al. 2021).

Furthermore, the genome of FPV-like viruses has been isolated from dogs with diarrhea, and the genomes of other symptoms are similar or identical to those of FPV (Wang et al. 2022). FPV-like viruses have become widespread in China and affect the health of dogs, but feline-derived FPV has not been reported to be infective in dogs. Since dogs and cats are the most common companion animals in China, potential cross-species infectious diseases have drawn great public concern. CPV resulting from FPV has posed a severe threat to dogs for several decades (Kelly 1978). Therefore, it is crucial to closely monitor and investigate the potential of FPV to infect dogs through further evolution and adaptation.

In this study, we carried out etiological surveillance of FPV in cats or kittens with diarrhea or vomiting symptoms from animal hospitals in parts of China. FPV strains with a wide range of prevalence and distant relationships from Cu-4 strain were selected through an evolutionary analysis of VP2 proteins for isolation. Based on amino acid differences in VP2 protein, we selected a specific FPV isolate to explore its clinical pathogenicity. This study provides a theoretical basis for the development of related drugs and vaccines against diseases caused by FPV infection.

Results

The infection rate of feline panleukopenia virus (FPV) is high in China

In this study, 746 gastrointestinal swab samples were collected from 18 provinces in China between 2018 and 2021. FPV was tested positive in the samples from 15 out of these 18 provinces, with detection rates varied (Fig. 1A). A nationwide cat FPV infection was observed, with an overall percentage of 45.4% (339/746, Fig. 1B). Moreover, a higher proportion of male cats (55.5%) were affected than female cats (44.5%). Cats older than ten months of age (34.7%) were less susceptible to FPV than were those younger than ten months (65.3%). FPV infection was lower in cats living alone (40.4%) than in those living in groups (≥ 2 cats, 59.6%). In pet hospitals, 80.8% of the cats with gastrointestinal (GI) symptoms were infected by FPV (Fig. 1C). The full-length FPV VP2 gene sequence of all positive samples was amplified using the primer pair VP2-F and VP2-R, and 65 unique sequences were obtained. A comparison of the nucleotide sequences of these VP2 genes revealed that six sequences (FPV-6, FPV-10, FPV-15, FPV-251, FPV-271 and FPV-S2) had the highest occurrence frequency in China's widely prevalent FPV-positive samples (Fig. 1D). The clinically relevant information of the six isolated FPV strains corresponding to these six sequences is presented in Table 1.

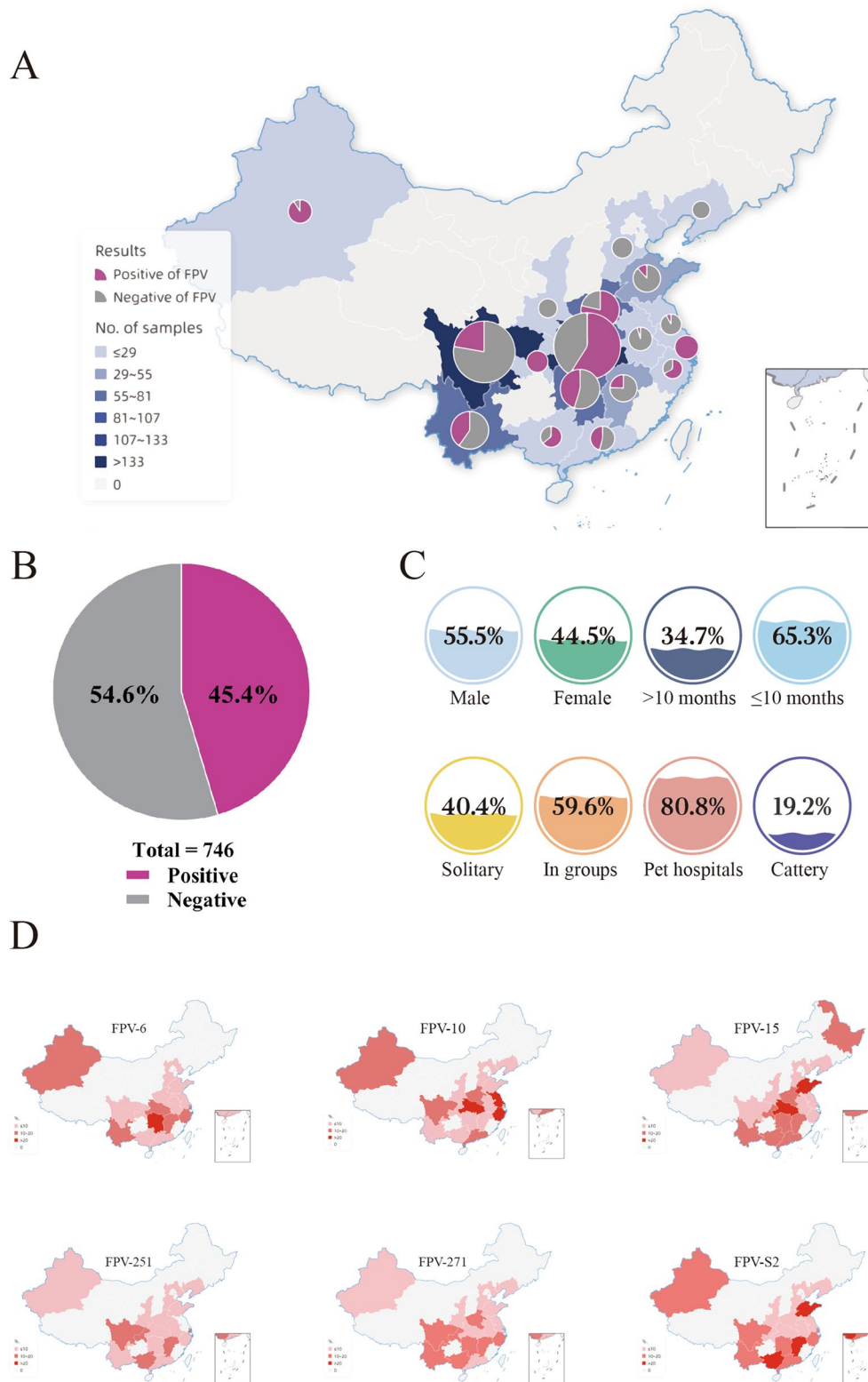


Fig. 1 Surveillance of FPV infection in selected regions of China, 2018-2022. **A** Locations of sample collection and FPV-positivity rate in each province. A darker color indicates a greater number of samples, and the pie charts show the percentages of positive and negative FPVs for each province. **B** Total detection rate of FPV. **C** The proportion of each component under different classifications of FPV-positive samples. **D** Share of the six FPV VP2 types with the highest prevalence in each province of FPV-positive samples. Sensor code of this map: GS (2019) 1695

Table 1 Information on samples corresponding to six VP2 gene sequences and the main clinical symptoms of FPV patients

VP2 gene sequences	Clinical symptoms	Regression	Region of China	GenBank No.
FPV-6	Diarrhea, fever, vomiting	Death	Hubei	OQ815870
FPV-10	Slight diarrhea	Rehabilitation	Henan	OQ815871
FPV-15	Diarrhea	Death	Jiangsu	OQ815872
FPV-251	Diarrhea, vomiting	Death	Sichuan	OQ815873
FPV-271	Diarrhea	Remission	Hebei	OQ815874
FPV-S2	Diarrhea, hematochezia	Death	Xinjiang	OQ815875

More than half of the common FPV strains in China may be distantly related to vaccine strain Cu-4

Phylogenetic analysis was performed for the obtained 65 VP2 gene sequences in this study, and 40 FPV strains isolated from China, 51 FPV strains from other countries, as well as previously reported sequences in the NCBI database (<https://www.ncbi.nlm.nih.gov/nucleotide/>). We found that the maximum likelihood (ML) phylogenetic tree of VP2 gene exhibited two clades. Clade 1 contained only four strain sequences from this study and one strain sequence from Korea (GenBank: MN400980.1). The majority of the FPV strain sequences were in clade 2, which was also subdivided into two subbranches (clades 2-1 and 2-2). Notably, the vaccine strain Cu-4 was in clade 2-1, and 33 VP2 were in clade 2-2 (33/65, 50.8%), which indicated that more than half of the circulating strains in China might have a distant genetic relationship with the vaccine strain Cu-4 (Fig. 2A). Furthermore, there was no significant regional variability in FPV based on the VP2 phylogenetic analysis.

Therefore, we selected six FPV-positive samples corresponding to VP2 gene sequence (four sequences in clade 2-2 and two sequences in clade 2-1) and successfully obtained six FPV isolates through observation of cytopathic effects (CPEs), FPV isolate-specific indirect immunofluorescence analysis (IFA), and transmission electron microscopy (TEM) (Fig. 2B).

VP2 protein of FPV isolates had several unique amino acid substitutions

The 156 full-length amino acid sequences of VP2 were employed to generate a probability map of variation (65 sequences in this study and 91 sequences in NCBI; Fig. 3). DNASTAR was used to translate and compare the six VP2 genes. The results showed that these FPV isolates differed at 11 amino acid residue sites in VP2 (Table 2). As shown in Fig. 3, Val83Ile, Thr101Ile, Ile232Val, His234Tyr, Glu411Ala and Val562Ala were six common substitutions, and another five substitutions, Ser140Arg (S140R), Val153Gly (V153G), A300P, Val308Ser (V308S) and Ala328Val (A328V) have not been reported or uploaded to the NCBI GenBank.

Substitutions S140R, V153G and A328V were included in FPV-10 (Table 2). BLAST analysis revealed that mink enteritis virus (MEV; GenBank, AAA47165.1) was most closely related to the FPV-10 strain and that FPV-10-infected cats exhibited mild diarrhea and recovered after 3-6 d (Table 1). Although the V308S substitution was found in VP2 gene of FPV-15 isolate, no report indicating that this substitution could cause a change in the function or properties. Variation at the 300th amino acid residue site in VP2 has been reported to affect the host selection range for picornaviruses (Allison et al. 2016). In addition, VP2 sequence of FPV-251 differs from that of FPV-271 only at the 300th amino acid residue site (A300P), which has been reported to correlate with the ability of viruses to infect cells (Parker and Parrish 1997). Therefore, we subsequently investigated FPV-251, VP2 protein of which has the substitution A300P.

Substitution of A300P increases the area of “spikes” on the surface of VP2 protein

We examined the A300P substitution in VP2 protein based on GenBank data of the amino acid substitution at the 300th site of VP2 in different *Protoparvoviruses* isolated from various hosts. We found that the amino acid residue at site 300 of VP2 protein is predominantly glycine in CPV, valine in blue fox parvovirus (BFPV) and MEV, and alanine in FPV. We also observed that the BFPV strain isolated from the blue fox (*Canidae*) had the same amino acid residue at site 300 of VP2 as the FPV-251 isolate (Table 3).

Molecular structure of VP2 protein of FPV-251 was predicted by SWISS-MODEL (<https://swissmodel.expasy.org/>), and a comparative analysis of A300P was performed using PyMOL. The results showed that, compared with conventional FPV (300-Ala), FPV-251 (300-Pro) had an additional topology (Fig. 4A), thus increasing the area of “spikes” on the surface of VP2 protein (Fig. 4B), which often influences host recognition and antigenicity (Hafenstein et al. 2009). Furthermore, we observed that FPV-271 (300-Ala) differed from FPV-251 (300-Pro) only at site 300 of VP2. Therefore, we used

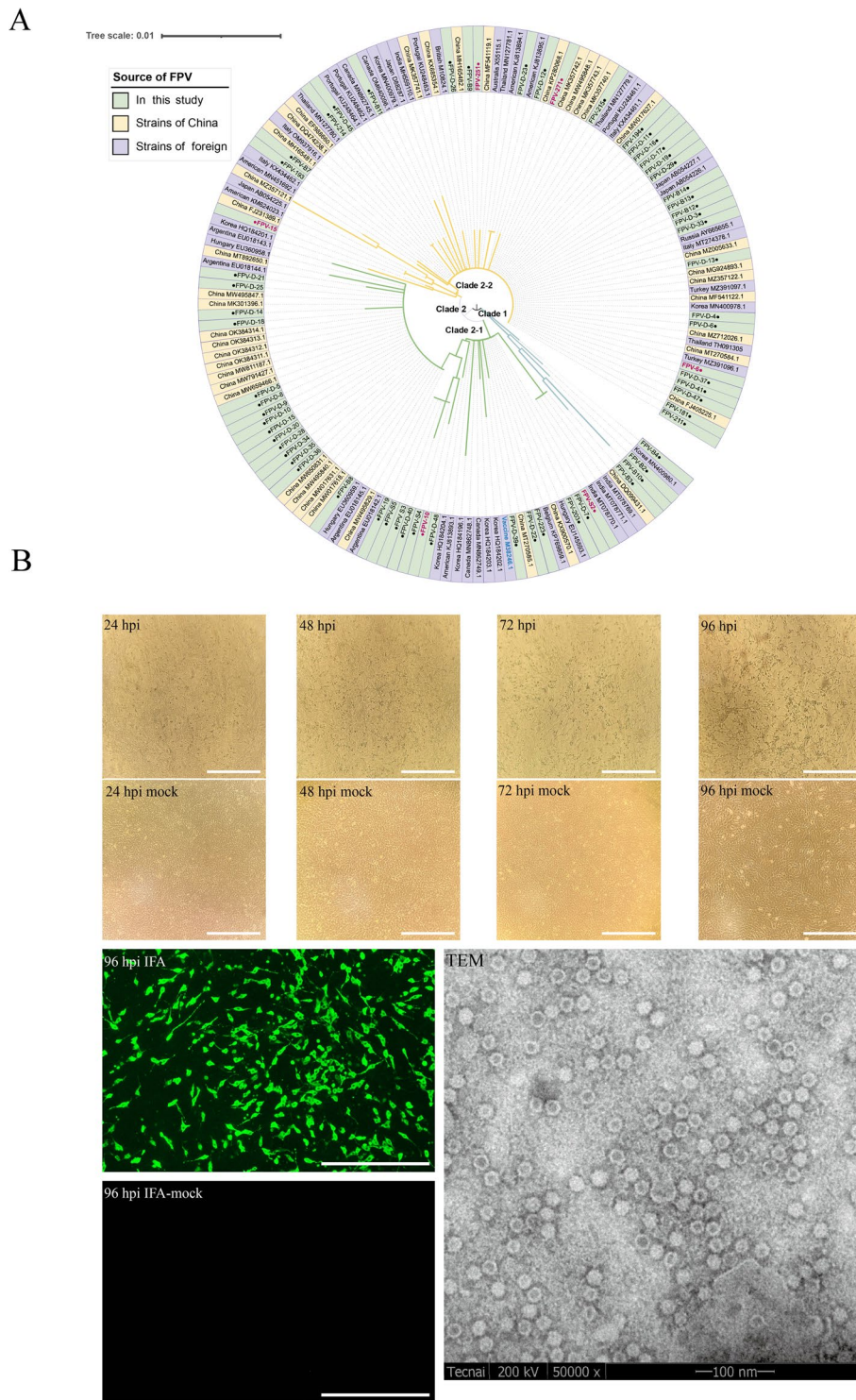


Fig. 2 Phylogenetic analysis, isolation, and identification of FPV in this study. **A** VP2 nucleotide sequence-based phylogenetic tree of 65 new sequences and reference sequences retrieved from GenBank. VP2 gene sequences from this study are marked in black “●” with a green background, and 91 VP2 gene sequences from NCBI are marked in bold red, and the vaccine strain is marked in bold blue. **B** Isolation and identification of six FPV isolates. CPEs were observed every 24 h post FPV-251 infection (hpi) in F81 cells (200×); FPV-251 isolate-specific IFA (green fluorescence) was performed on F81 cells at 96 hpi (200×); and FPV-251 virions were observed under a transmission electron microscope (Scale bar = 100 nm)

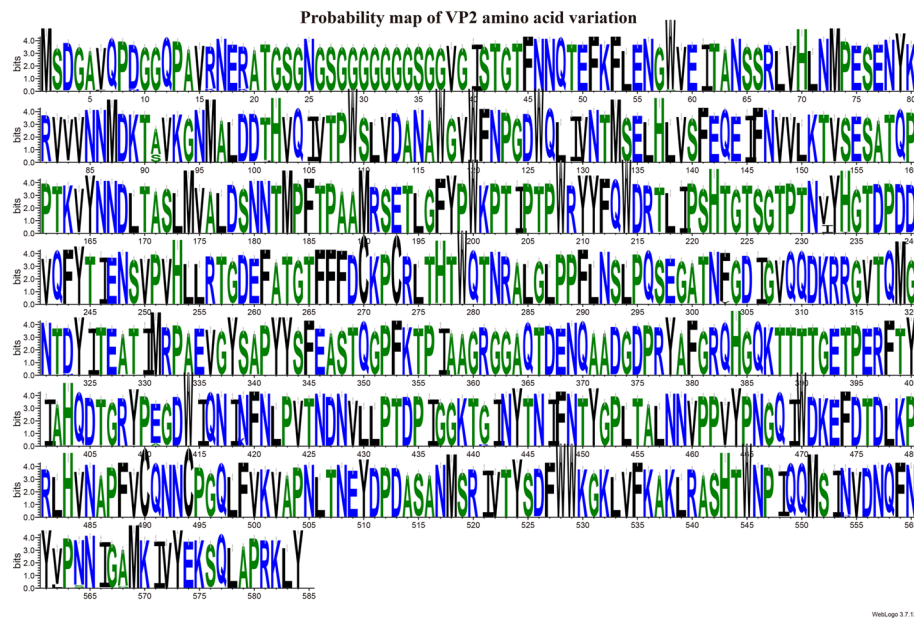


Fig. 3 Probability map of VP2 amino acid substitutions. The size of the graphic character at the corresponding site is proportional to the occurrence frequency of amino acids at a certain site

Table 2 Differences in the amino acid profile of six FPV isolates

Isolates	VP2 amino acid sites										
	83	101	140	153	232	234	300	308	328	411	562
FPV-6	V	I	S	V	I	H	A	V	A	E	V
FPV-10	I	T	R	G	I	Y	A	V	V	E	V
FPV-15	V	T	S	V	V	H	A	S	A	E	V
FPV-251	V	T	S	V	I	H	P	V	A	A	L
FPV-271	V	T	S	V	I	H	A	V	A	A	L
FPV-S2	V	T	S	V	V	H	A	V	A	E	V

the FPV-271 isolate as a control strain for investigating the host range substitution of FPV-251.

FPV-251 isolate can replicate stably in canine cell lines

Previous studies have suggested that FPV cannot replicate or replicate only slightly in canine cell lines such as MDCK cells and A72 cells (Horiuchi et al. 1992). However, our data showed that FPV-251 can efficiently propagate in MDCK (Fig. 5A) and A72 cells (Fig. 5B), which exhibit viral titers > 10⁵ tissue culture infectious doses of 50% per milliliter (TCID₅₀/mL). In contrast, FPV-271 does not exhibit similar propagation capabilities. Both FPV isolates replicated relatively well in the feline kidney fibroblast-like monolayer cell line (F81 cells) (Fig. 5C), with FPV-251 replicating significantly more efficiently than FPV-271. All the viruses were passaged three times in culture on F81 cells.

FPV-251 and FPV-271 isolates have similar feline pathogenicity

When cats were orally infected with FPV-251 or FPV-271, they exhibited obvious clinical signs in the gastrointestinal tract (such as diarrhea and vomiting). The fecal scores at 0 d post inoculation (0 dpi), 3 dpi, 6 dpi and 9 dpi are shown in Fig. 6A. On the other hand, we observed that all anal swabs in FPV-251 and FPV-271 cat groups displayed a viral load of no less than 10^{3.0} TCID₅₀/mL at 3 dpi, except for those in the control cat group (Fig. 6B). At the end of the observation period (14 dpi), all cats were euthanized and autopsied. Hematoxylin-eosin (H&E) staining revealed obvious mesenteric lymph node hemorrhage and intestinal villus shedding in the FPV-251 and FPV-271 cat groups, but no abnormalities were found in the control cat group (Fig. 6C). Immunohistochemical (IHC) staining revealed the presence of brown-stained FPV particles in the gastrointestinal

Table 3 Variation in amino acid composition at residue 300 in different parvoviruses and host information statistics

Virus	Strains	VP2 300 amino acid	Host	GenBank No.
FPV	FPV-251	P	Cat	OQ815873
	Cu-4	A	Cat	M38246.1
	Philips Roxane	A	Dog	M24002.1
	Giant panda/CD/2018	A	Giant panda	MW091487.1
	MHS2019	A	South China Tiger	MN908257.1
	monkey/BJ 22/2008/CHN	A	Monkey	FJ231389.1
BFPV	BFPV	V	Vulpes lagopus	MN451652.1
	BFPV-1	V	Alopex lagopus	U22185.1
	BFPV	P	Blue Fox	GQ857595.1
CPV-2	F2016020	A	Cat	MH329287.1
CPV 2a	CPV02	G	Canis lupus familiaris	MW889096.1
CPV new 2a	CPV new 2a variant	G	Dog	MN661243.1
CPV 2b	FR1/CPV2-2021-HUN	G	Dog	ON733252.1
CPV new 2b	CPV-BM(11)	G	Dog	JQ743894.1
CPV 2c	CPV12	G	Canis lupus familiaris	MW889106.1
MEV	MEV-LHV	V	Mink	KT899745.1
	MEV-SD8	V	Mink	KY094119.1
	JL	V	Mink	MT250783.1

tracts and MLNs (Fig. 6C). In summary, both FPV-251 and FPV-271 can infect cats orally and replicate efficiently in the intestine, thus causing enterocolitis.

FPV-251 isolate is pathogenic to dogs

It is difficult to obtain blue foxes in China, and the chance of blue foxes being wild animals contacting pet cats is low; therefore, we explored whether the FPV-251 isolate can infect dogs (Huang et al. 2021a). The fecal scoring results showed that three out of the five dogs in the FPV-251 dog group had scores of 1, two dogs had a score of 2, at 0 dpi, 3 dpi, 6 dpi, and 9 dpi. In contrast, the FPV-271 dog group and the control dog group had normal fecal scores (0) (Fig. 7A). It should be noted that dogs in the FPV-251 dog group exhibited severe diarrhea symptoms at 6 dpi, with an FPV titer of $\geq 10^{4.0}$ TCID₅₀/mL according to their anal swabs, whereas FPV was not detected in either the FPV-271 dog group or the control dog group (Fig. 7B).

Autopsy of the tested dogs revealed that FPV-251 infection caused enteritis, redness and congestion of the intestines, and swelling of the MLNs. H&E staining showed severe intestinal villous disintegration and hemorrhage of the MLNs in the FPV-251 dog group. IHC illustrated brown-stained virus particles in the dog intestinal tract and in the MLNs of the FPV-251 dog group, and these tissues were identified as FPV-251 isolates by PCR (Fig. 7C). In contrast, in the FPV-271 dog group and control dog group, the dog tissues and organs presented no abnormalities, well-arranged

intestinal villi were also observed under the microscope, and there were no stained virus particles in cells (Fig. 7C). Taken together, these findings suggest that FPV-251 can replicate in the canine intestine and cause intestinal abnormalities.

Discussion

In this study, it is the first time to identify an A300P substitution in VP2 protein in cat-derived FPV. We further performed protein structure analysis and found that VP2 protein structure of FPV-251 was slightly altered in the presence of the A300P substitution. These small surface differences at or near capsid amino acids might be associated with the observed in vitro cell tropism and in vivo pathogenic properties of the viruses (Agbandje et al. 1993). According to the epidemiological investigation of FPV, the overall percentage of FPV-positive individuals was 45.4%, which was slightly lower than that reported by Miranda C in Portugal but significantly higher than that reported in other studies (Balboni et al. 2018; Liu et al. 2020; Miranda et al. 2017; Ndiana et al. 2022). Additionally, cats living in groups had a higher FPV positivity rate than cats living alone, possibly because the prevalence of FPV tends to be density dependent (Loock et al. 2018).

Moreover, no significant regional variability in FPV was found *via* VP2 gene-based genetic evolutionary analysis. The possibly underwent a variety of substitutions under

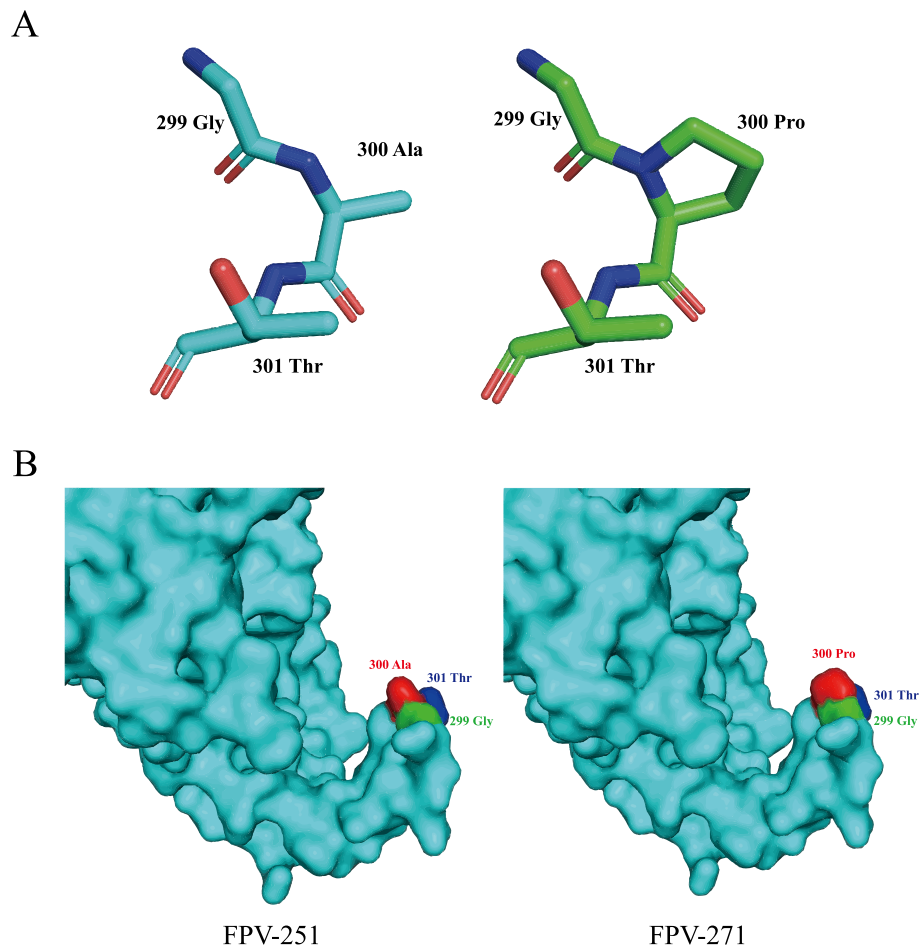


Fig. 4 Effects of substitutions at VP2 amino acid residue 300 (A300P) on protein tertiary structure. **A** Diagram of the substitution structure model. **B** Structural changes after tertiary structural substitution of VP2 protein

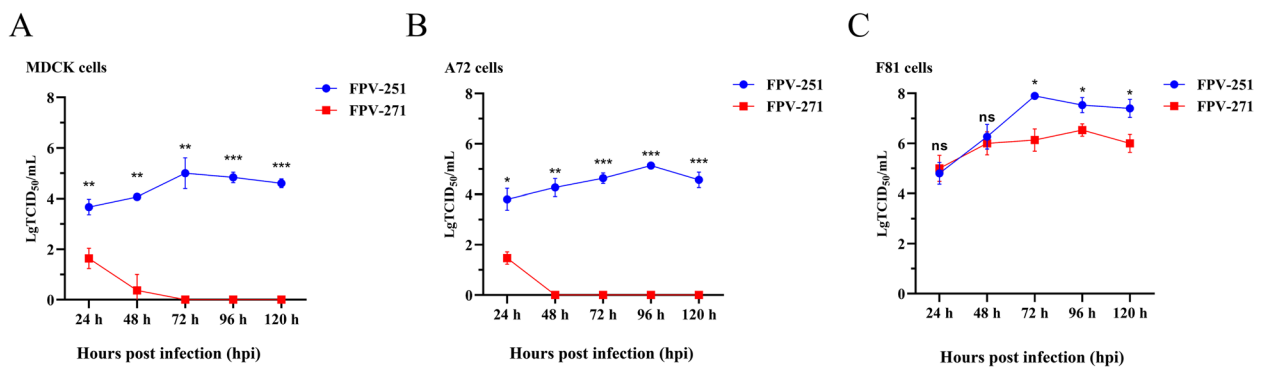


Fig. 5 Comparison of the replication ability of FPV-251 and FPV-271 in different cells. **A** MDCK cells. **B** A72 cells. **C** F81 cells

vaccine-driven selection (Wen et al. 2018), leading to an increase of the ability to evade the immune surveillance, as well as expand the range of host selection (Kang et al. 2017; Truyen et al. 1994). It has been reported that surface residues in the “shoulder” region of the threefold

spikes adjacent to the VP2 residue site 300 (the “300 region”) play an important role in host range determination (Parker and Parrish 1997). A300P was originally found only in BFPV isolated from blue foxes (China, GenBank: GQ857595). Blue foxes belong to the canine

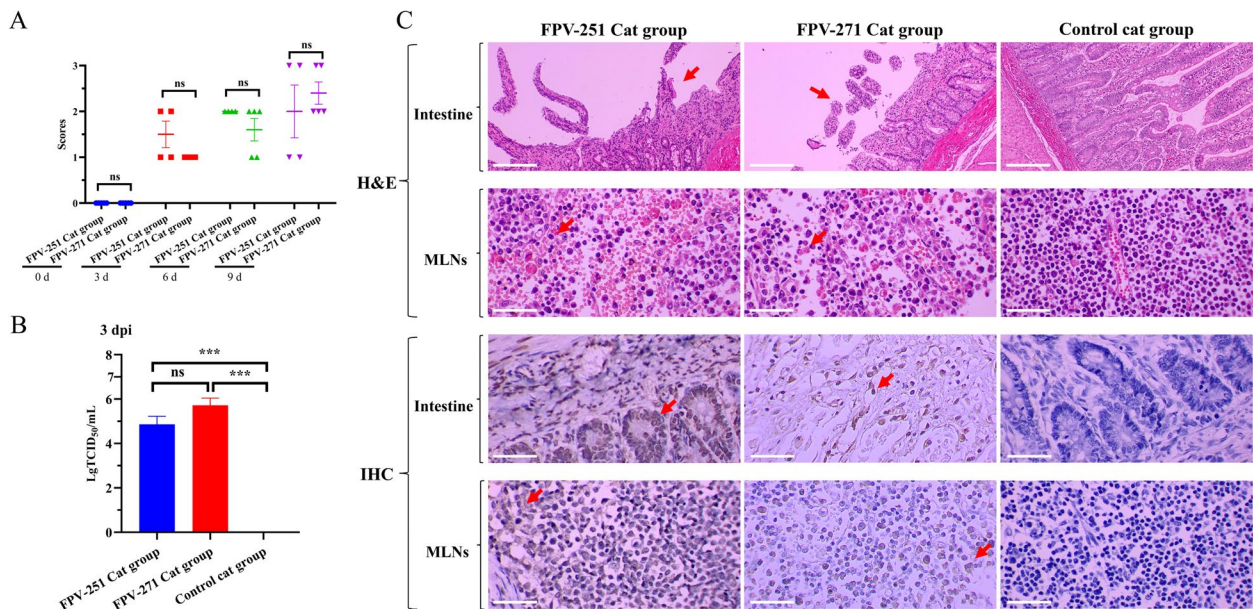


Fig. 6 Observations of cat indicators after FPV-251 and FPV-271 infection. **A** Fecal scores for the cats at 0 dpi (day post inoculation), 3 dpi, 6 dpi and 9 dpi. **B** FPV levels in anal swabs of each test cat at 3 dpi (50% tissue culture infective dose). **C** H&E staining and IHC staining of intestine and MLN tissues from test cats in each group. Scale bars of H&E staining for Intestine = 200 μm. Scale bars of H&E staining for MLNs = 60 μm. Scale bars of IHC staining = 60 μm

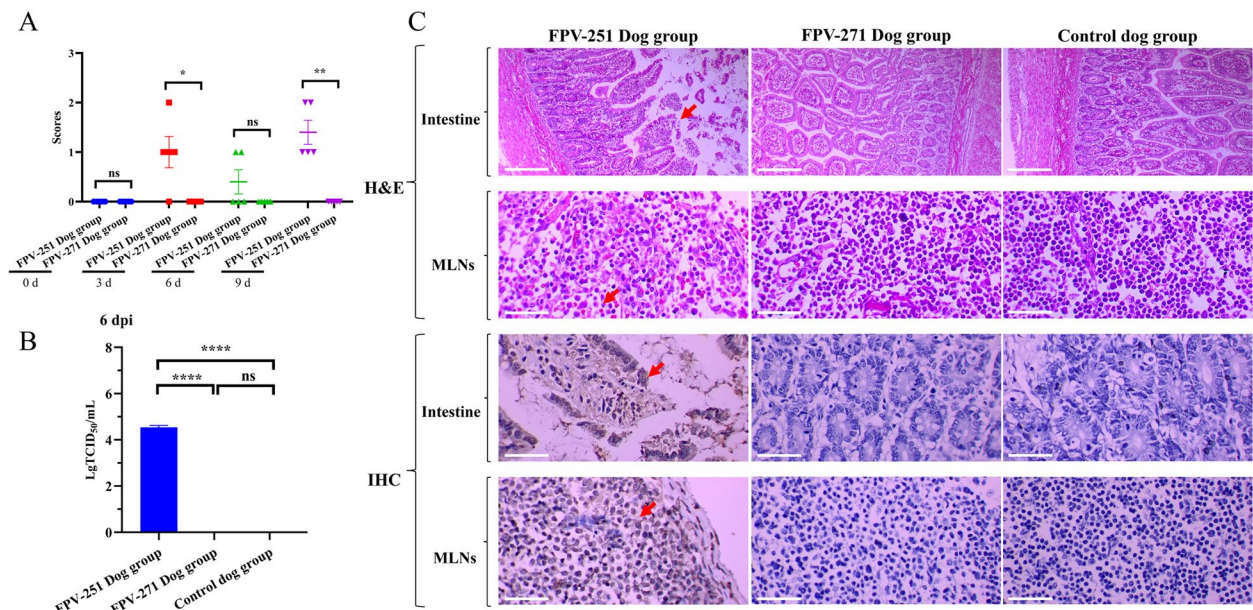


Fig. 7 Observations of dog indicators after FPV-251 and FPV-271 infection. **A** Fecal scores for the FPV-251 Dog group, FPV-271 Dog group and Control Dog group. **B** FPV levels in the anal swabs of each test dog at 6 dpi (50% tissue culture infective dose). **C** H&E staining and IHC staining of intestine and MLNs from test dogs in each group. Scale bars of H&E staining for Intestine = 200 μm. Scale bars of H&E staining for MLNs = 60 μm. Scale bars of IHC staining = 60 μm. dpi: day post inoculation

family, and we considered whether A300P could lead FPV to develop a different cellular tropism, such as in a canine cell line.

As expected, FPV-251 replicated efficiently and stably (but at no more than $10^{5.0}$ TCID₅₀/mL) in both MDCK and A72 cells, which challenged the view that FPV cannot proliferate efficiently on canine cell lines (Diakoudi et al. 2022;

Horiuchi et al. 1992; Truyen and Parrish 1992). Notably, a virus highly similar to the feline panleukopenia virus (also known as FPV-like virus) has been isolated from dogs with gastrointestinal disease. This FPV-like virus can infect dogs, cause severe clinical symptoms and replicate efficiently in MDCK cell lines (Wang et al. 2022). FPV-like viruses have become widespread worldwide. For example, they are common in dogs in South America (Bucafusco et al. 2019). In addition, our findings demonstrated that the FPV-251 strain, initially isolated from cats, can induce disease in dogs. This may result in an evolutionary trend in FPV progression toward infecting dogs, which is particularly evident under vaccine-induced selective pressure. In recent years, the number of domestic cats and dogs has increased dramatically, and this newly discovered interspecies transmissible FPV strain could pose a significant threat to households that cohabit both cats and dogs. Furthermore, cat-carried zoonotic pathogens such as SARS-CoV-2 and feline rotavirus (FRV) have become increasingly important for humans (Gauchan et al. 2015; Yang et al. 2021). Thus, FPV evolution deserves attention and surveillance (Parker et al. 2001).

As discussed earlier, FPV-251 has evidently acquired infectivity and pathogenicity in dogs. It is well documented that canine parvovirus (CPV) can cause severe clinical manifestations and high mortality rates, exceeding 50%, in dogs. Notably, CPV is believed to have evolved from FPV (Kelly 1978). In light of the suggested speculation in this study that a mutation in the 300th amino acid of VP2 protein may result in a modification in the cytophilicity of FPV, we also evaluated this site within CPV. Interestingly, this residue is predominantly occupied by glycine in CPV, which significantly contrasts with the prevalence of alanine at the same position in FPV. In summary, the 300th amino acid variation may impact critical regions responsible for viral entry, receptor binding, or host cell interactions.

Although our study reveals several important discoveries, it has several limitations. First, our sample was limited to cats with clinical GI symptoms, and many cats with invisible FPV infections were excluded; therefore, our FPV-positive rate represented only the FPV apparent infection rate rather than the complete FPV positivity rate in Chinese domestic cats. Second, VP2 protein accounts for 90% of the capsid protein of FPV, and it plays a crucial role in viral entry into cells, replication, and antigenicity. Therefore, this study focused mainly on VP2 protein of FPV, and potential functions of the nonstructural proteins NS1 and NS2 and the structural protein VP1 were overlooked. Despite the abovementioned limitations, our findings provide insight into the transmission route and host range of FPV and offer a valuable reference for the formulation of preventive strategies. Although our study identified a cat-derived FPV isolate that is capable of

causing disease in dogs, further investigation is needed to determine whether the replacement of alanine with proline at position 300 of VP2 protein is responsible for this difference.

Conclusion

This study reported the high prevalence of FPV in China and revealed that one of the feline-derived FPV isolates, FPV-251, has a special variation at the 300th amino acid residue in VP2 protein (alanine was replaced by proline). Moreover, this study showed that FPV-251 is pathogenic to dogs.

Methods

Sample collection

A total of 746 anal swab samples were collected from animal hospitals in 18 provinces of China from 2018 to 2022, and all the sampled cats had digestive tract diseases (diarrhea or vomiting). For each sample collection, the sampling areas were chosen based on the representative city or region and the convenience of transportation to ensure that the samples would be transported to the laboratory within 72 h after sampling. The swab samples were placed in 1 mL of sterile transport medium (Dulbecco's modified Eagle's medium (Gibco) containing 100 IU/mL penicillin, 100 µg/mL streptomycin, and 2% newborn calf bovine serum (NBS, Gibco)). The tissue samples were submerged in the transport medium and subsequently ground. After collection, the samples were placed on ice and transported to the laboratory within 72 h.

Identification of FPV-positive samples

DNA extraction from the swabs was performed with a Fast-Pure Viral DNA/RNA Mini Kit (Cat. No: RC311) purchased from Vazyme Biotech Co., Ltd. (Nanjing, China). The identification primers used were designed using Oligo 6 according to the sequence of the reference strain FPV-BJ05 (GenBank: MH165482.1) in the NCBI database (<https://www.ncbi.nlm.nih.gov/nucleotide/>). The primer pair F1 (5'-CAAATA GAGCATTGGGCTTACC-3') and R1 (5'-TCGGGTGTT TCTCCTGTTGTAG-3') was used to amplify a 344-bp fragment of the partial VP2 gene of FPV. Conventional PCR was performed using 2× Accurate Taq Master Mix (dye plus) (Hunan Accurate Bioengineering Co., Ltd., China) according to the manufacturer's instructions.

Virus isolation and sequencing

To further analyze the genetic characteristics of the FPV-positive samples, the full-length sequence of VP2 gene was amplified using another primer pair, VP2-F (5'-AGG ACAAGTAAAGAGACAATC-3') and VP2-R (5'-GTA TATATAATTTTCTAGGTGCT-3'), which was designed in reference to the NCBI database to obtain a 1,800 bp

amplicon. The resulting sequences were assembled and edited with the SeqMan software package of the DNASTar package and subsequently aligned to the FPV strain sequence from the GenBank database (<http://www.ncbi.nlm.nih.gov/>). All nucleotide sequences obtained from the samples in this study were aligned to 90 other reference FPV strain sequences and 1 vaccine Cu-4 strain sequence (GenBank: M38246.1) from the GenBank database. A maximum likelihood (ML) phylogenetic tree was constructed by the neighbor-joining method using MEGA7 with 1,000 bootstrap replicates (Huang et al. 2021b).

FPV samples were filter-sterilized *via* 0.22 µm filtering film (EMD Millipore, Billerica, MA, USA) to obtain FPV samples evolutionarily distant from the Cu-4 strain. The filtered supernatants were subsequently inoculated into F81 cells. CPEs were observed daily under an inverted microscope until they reached 80%. Cultures were harvested and centrifuged (at 5,000 rpm for 30 min at 4°C), and the supernatants were processed immediately or stored at -80°C in 1 mL aliquots.

FPV isolates were identified using an indirect immunofluorescence assay (IFA). Specifically, F81 cells infected with FPV (F81/FPV) were fixed with 80% acetone for 10 min, incubated with a mouse monoclonal primary antibody against FPV VP2 for 1 h at 37°C, and incubated with a FITC-conjugated goat polyclonal secondary antibody against mouse IgG-H&L (Alexa Fluor® 488, Abcam, USA) for 45 min at room temperature for IFA. After each step, F81/FPV was washed three times for 5 min each with PBST (phosphate buffer saline with 0.05% Tween-20). Finally, the cells were observed under a fluorescence microscope.

The CPE cell cultures were centrifuged at 30,000×g for 10 min, negatively stained with 0.2% phosphotungstic acid, and observed *via* TEM.

Virus titer assays

We evaluated virus titers by the 50% tissue culture infective dose (TCID₅₀) assay. F81 cells were seeded in 96-well plates in DMEM supplemented with 5% NBS. The virus samples were serially diluted 10-fold with DMEM and inoculated into F81 cells at 37°C for 120 h. IFA was performed to determine whether the virus was infecting F81 cells, and the TCID₅₀ was calculated *via* the Reed–Muench method.

Verification of FPV-251 and FPV-271 pathogenicity in cats

The experimental cats were identified as negative for FPV by PCR and IFA. Three-week-old domestic cats ($n=15$) were randomly divided into three groups (the FPV-251 cat group, FPV-271 cat group, and control cat group), with five cats per group. Five cats from each group lived in a single animal house (3.2 m × 3.2 m). Each cat in the FPV-251 cat group was orally inoculated with 1 mL (10^{7.5}

TCID₅₀/mL) of the FPV-251 isolate, that in the FPV-271 cat group was inoculated with 1 mL (10^{7.5} TCID₅₀/mL) of the FPV-271 isolate, and that in the control cat group was inoculated with equal volumes of DMEM. Cats were observed and evaluated daily for clinical signs until 14 dpi (Janke et al. 2022). Fecal scoring was recorded every three days using a 4-tiered system until 9 dpi, with 0 = normal feces, 1 = soft but formed feces, 2 = semifluid feces, and 3 = watery diarrhea. We performed a double-blind (participant and assessor) evaluation to avoid significant bias introduced to the clinical scoring. Anal swabs were collected every day to determine viral shedding. At 14 dpi, all of the cats were euthanized according to the protocol suggested by the World Society for the Protection of Animals, Methods for Euthanasia of Dogs and Cats (<https://www.rspca.org.uk/>).

Analysis of FPV-251 and FPV-271 pathogenicity in dogs

The experimental dogs were identified as negative for FPV by PCR and IFA. Three-week-old domestic dogs ($n=15$) were randomly divided into three groups (the FPV-251 dog group, FPV-271 dog group, and control dog group), with five dogs per group. Five dogs from each group lived in a single animal house (3.2 m × 3.2 m). In the FPV-251 dog group, 1 mL (10^{7.5} TCID₅₀/mL) of the FPV-251 isolate was orally inoculated; in the FPV-271 dog group, 1 mL (10^{7.5} TCID₅₀/mL) of the FPV-271 isolate was inoculated; and in the control dog group, equal volumes of DMEM were inoculated. Dogs were observed and evaluated daily for clinical signs until all animals were clinically free or dead. The methods used for fecal scoring, double-blind evaluation, anal swab collection, and mercy killing were the same as those used for the cats.

Data analysis

We applied an online map-making tool to perform statistical analysis of the sample data and test results (<https://dycharts.com/appv2/#/pages/home/index>). GraphPad Prism 9 software was used for graphing and significance analysis of the data. The DNASTar package (V. 7.1.0) was used to cut, assemble, and save all DNA sequences. MEGA V. 7.0.14 was used to perform genetic evolutionary analysis of VP2 gene sequences, and online tools were used to construct and modify the evolutionary tree (<https://itol.embl.de/>). SWISS-MODEL (<https://swissmodel.expasy.org/>) and PyMOL were used to predict and analyze the protein tertiary structure, respectively. The data were graphed and statistically analyzed using GraphPad Prism V. 9 software. The results are reported as the mean ± standard deviation (SD) from a minimum of three independent experiments. Statistical significance was determined using Student's two-tailed unpaired t test (ns, $p > 0.05$; *, $p < 0.05$; **, $p < 0.01$; ***, $p < 0.001$).

Abbreviations

Ala300Pro, A300P	Replacement of alanine with proline at position 300 th of the VP2 protein
A72 cells	Canine fibrosarcoma (A72) cell
BFPV	Blue fox parvovirus
CPV	Canine parvovirus
CPEs	Cytopathic effects
dpi	Day post inoculation
FCV	Feline calicivirus
FeLV	Feline leukemia virus
FPV	Feline panleukopenia virus
FRV	Feline rotavirus
F81 cells	Feline kidney fibroblast-like monolayer cell line
GI symptoms	Gastrointestinal symptoms
hpi	Hours post infection
H&E	Hematoxylin-eosin
IFA	Indirect immunofluorescence analysis
MDCK	Madin-Darby canine kidney
MEV	Mink enteritis virus
ML	Maximum likelihood
MLNs	Mesenteric lymph nodes
NBS	Newborn Calf Bovine Serum
NS1	Non-structural protein 1
NS2	Non-structural protein 2
ORFs	Open reading frames
TCID ₅₀ /mL	tissue culture infectious dose 50% per milliliter
TEM	Transmission electron microscopy
VLP	virus-like particle
VP2	Capsid (virion) protein 2

Acknowledgments

Not applicable.

Authors' contributions

Jiakang Li, Shengbo Cao, and Qiuyan Li designed the experiments, interpreted the data and wrote the article. Jiakang Li, Jiajia Peng, Yue Zeng, Ying Wang, and Luying Li performed the experiments with assistance and advice from Yiran Cao, Dengyuan Zhou, Longlong Cao and Qingxiu Chen. Zijun Ye and Jiajia Peng were responsible for collecting the swab samples. All the authors read and approved the final manuscript.

Funding

This work was supported by the Experimental Animal Research Project of Hubei Province (Grant No. 2023CFA005).

Availability of data and materials

The datasets used or analyzed during the current study are available from the corresponding author upon reasonable request.

Declarations

Ethics approval and consent to participate

In this study, all of the felines and canines used in this study were maintained in compliance with the recommendations of the Regulations for the Administration of Affairs Concerning Experimental Animals established by the Ministry of Science and Technology of China. The experiments were performed using protocols that were approved by the Scientific Ethics Committee of Huazhong Agricultural University (permit number for cats: HZAUCA-2023-0036; permit number for dogs: HZAUDO-2023-0017). The samples collected also followed the approved animal practices of the Scientific Ethics Committee of Huazhong Agricultural University (permit number: HZAUCA-2018-002).

Consent for publication

The authors approved the publication of the manuscript.

Competing interests

The authors declare that there are no conflicts of interest associated with this manuscript. The author Shengbo Cao was not involved in the journal's review or decisions related to this manuscript.

Author details

¹National Key Laboratory of Agricultural Microbiology, Huazhong Agricultural University, Wuhan 430070, Hubei, China. ²Laboratory of Animal Virology, College of Veterinary Medicine, Huazhong Agricultural University, Wuhan, Hubei, P. R. China. ³Wuhan Keqian Biology Co., Ltd, Wuhan, Hubei, P. R. China. ⁴Department of Life Science, Imperial College London, London, UK.

Received: 1 November 2023 Accepted: 11 December 2023

Published online: 29 January 2024

References

- Agbandje, M., R. McKenna, M.G. Rossmann, M.L. Strassheim, and C.R. Parrish. 1993. Structure determination of feline panleukopenia virus empty particles. *Proteins* 16: 155–171. <https://doi.org/10.1002/prot.340160204>.
- Allison, A.B., L.J. Organtini, S. Zhang, S.L. Hafenstein, E.C. Holmes, and C.R. Parrish. 2016. Single mutations in the VP2 300 loop region of the three-fold spike of the carnivore parvovirus capsid can determine host range. *Journal of virology* 90: 753–767. <https://doi.org/10.1128/JVI.02636-15>.
- Balboni, A., F. Bassi, S. De Arcangeli, R. Zobba, C. Dedola, A. Alberti, and M. Battilani. 2018. Molecular analysis of carnivore protoparvovirus detected in white blood cells of naturally infected cats. *BMC veterinary research* 14: 41. <https://doi.org/10.1186/s12917-018-1356-9>.
- Barrs, V.R. 2019. Feline panleukopenia: a re-emergent disease. the veterinary clinics of North America. *Small animal practice* 49: 651–670. <https://doi.org/10.1016/j.cvsm.2019.02.006>.
- Battilani, M., M. Bassani, D. Forti, and L. Morganti. 2006. Analysis of the evolution of Feline Parvovirus (FPV). *Veterinary Research Communications* 30: 223–226. <https://doi.org/10.1007/s11259-006-0046-4>.
- Bucafusco, D., H. Argibay, L. Diaz, C. Vega, L. Minatel, G.C. Postma, M. Rinas, and A. Bratanich. 2019. First characterization of a canine parvovirus causing fatal disease in coatis (*Nasua nasua*). *Archives of virology* 164: 3073–3079. <https://doi.org/10.1007/s00705-019-04417-4>.
- Cao, L., Q. Li, K. Shi, L. Wei, H. Ouyang, Z. Ye, W. Du, J. Ye, X. Hui, J. Li, S. Cao, and D. Zhou. 2022. Isolation and phylogenetic analysis of feline calicivirus strains from various region of China. *Animal Diseases* 2: 16. <https://doi.org/10.1186/s44149-022-00047-7>.
- Capozza, P., E. Lorusso, V. Colella, J.C. Thibault, D.Y. Tan, J.P. Tronel, L. Halos, F. Beugnet, G. Elia, V.L. Nguyen, L. Occhiogrosso, V. Martella, D. Otranto, and N. Decaro. 2021. Feline leukemia virus in owned cats in Southeast Asia and Taiwan. *Veterinary microbiology* 254: 109008. <https://doi.org/10.1016/j.vetmic.2021.109008>.
- Chowdhury, Q., S. Alam, M.S.R. Chowdhury, M. Hasan, M.B. Uddin, M.M. Hosain, M.R. Islam, M.M. Rahman, and M.M. Rahman. 2021. First molecular characterization and phylogenetic analysis of the VP2 gene of feline panleukopenia virus in Bangladesh. *Archives of virology* 166: 2273–2278. <https://doi.org/10.1007/s00705-021-05113-y>.
- Cotmore, S.F., and P. Tattersall. 1987. The autonomously replicating parvoviruses of vertebrates. *Advances in virus research* 33: 91–174. [https://doi.org/10.1016/s0065-3527\(08\)60317-6](https://doi.org/10.1016/s0065-3527(08)60317-6).
- Cotmore, S.F., M. Agbandje-McKenna, M. Canuti, J.A. Chiorini, A.M. Eis-Hubinger, J. Hughes, M. Mietzsch, S. Modha, M. Ogliastro, J.J. Pénzes, et al. 2019. Ictv Report 2019. ICTV Virus Taxonomy Profile: Parvoviridae. *The Journal of general virology* 100: 367–368. <https://doi.org/10.1099/jgv.0.001212>.
- Diakoudi, G., C. Desario, G. Lanave, S. Salucci, L.A. Ndiana, A.A.K. Zarea, E.A. Fouad, A. Lorusso, F. Alfano, A. Cavalli, C. Buonavoglia, et al. 2022. Feline Panleukopenia Virus in Dogs from Italy and Egypt. *Emerging infectious diseases* 28: 1933–1935. <https://doi.org/10.3201/eid2809.220388>.
- Gauchan, P., E. Sasaki, T. Nakagomi, L.P. Do, Y.H. Doan, M. Mochizuki, and O. Nakagomi. 2015. Whole genotype constellation of prototype feline rotavirus strains FRV-1 and FRV64 and their phylogenetic relationships with feline-like human rotavirus strains. *The Journal of general virology* 96: 338–350. <https://doi.org/10.1099/vir.0.070771-0>.
- Hafenstein, S., V.D. Bowman, T. Sun, C.D. Nelson, L.M. Palermo, P.R. Chipman, A.J. Battisti, C.R. Parrish, and M.G. Rossmann. 2009. Structural comparison of different antibodies interacting with parvovirus capsids. *Journal of virology* 83: 5556–5566. <https://doi.org/10.1128/JVI.02532-08>.
- Horiuchi, M., N. Ishiguro, H. Goto, and M. Shinagawa. 1992. Characterization of the stage(s) in the virus replication cycle at which the host-cell specificity

- of the feline parvovirus subgroup is regulated in canine cells. *Virology* 189: 600–608. [https://doi.org/10.1016/0042-6822\(92\)90583-b](https://doi.org/10.1016/0042-6822(92)90583-b).
- Huang, H., G. Yang, W. Zhang, X. Xu, W. Yang, W. Jiang, and X. Lai. 2021. A deep multi-task learning framework for brain tumor segmentation. *Frontiers in oncology* 11: 690244.
- Huang, J., Y. Liu, T. Zhu, and Z. Yang. 2021. The asymptotic behavior of bootstrap support values in molecular phylogenetics. *Systematic biology* 70: 774–785. <https://doi.org/10.1093/sysbio/syaa100>.
- Hueffer, K., L. Govindasamy, M. Agbandje-McKenna, and C.R. Parrish. 2003. Combinations of two capsid regions controlling canine host range determine canine transferrin receptor binding by canine and feline parvoviruses. *Journal of virology* 77: 10099–10105. <https://doi.org/10.1128/jvi.77.18.10099-10105.2003>.
- Janke, K.J., L.S. Jacobson, J.A. Giacinti, and J.S. Weese. 2022. Fecal viral DNA shedding following clinical panleukopenia virus infection in shelter kittens: a prospective, observational study. *Journal of feline medicine and surgery* 24: 337–343. <https://doi.org/10.1177/1098612X211023056>.
- Kang, H., D. Liu, J. Tian, X. Hu, X. Zhang, H. Yin, H. Wu, C. Liu, D. Guo, Z. Li, Q. Jiang, J. Liu, and L. Qu. 2017. Feline panleukopenia virus NS2 suppresses the host IFN- β induction by disrupting the interaction between TBK1 and STING. *Viruses* 9 (1): 23. <https://doi.org/10.3390/v9010023>.
- Kelly, W.R. 1978. An enteric disease of dogs resembling feline panleucopaenia. *Australian veterinary journal* 54: 593. <https://doi.org/10.1111/j.1751-0813.1978.tb02426.x>.
- Langeveld, J.P., J.I. Casal, C. Vela, K. Dalsgaard, S.H. Smale, W.C. Puijk, and R.H. Meulen. 1993. B-cell epitopes of canine parvovirus: distribution on the primary structure and exposure on the viral surface. *Journal of virology* 67: 765–772. <https://doi.org/10.1128/jvi.67.2.765-772.1993>.
- Liu, C., Y. Liu, P. Qian, Y. Cao, J. Wang, C. Sun, B. Huang, N. Cui, N. Huo, H. Wu, L. Wang, X. Xi, and K. Tian. 2020. Molecular and serological investigation of cat viral infectious diseases in China from 2016 to 2019. *Transboundary and emerging diseases* 67: 2329–2335. <https://doi.org/10.1111/tbed.13667>.
- Loock, D.J.E., S.T. Williams, K.W. Emslie, W.S. Matthews, and L.H. Swanepoel. 2018. High carnivore population density highlights the conservation value of industrialized sites. *Scientific reports* 8: 16575. <https://doi.org/10.1038/s41598-018-34936-0>.
- Miranda, C., M.J. Vieira, E. Silva, J. Carvalheira, C.R. Parrish, and G. Thompson. 2017. Genetic analysis of feline panleukopenia virus full-length VP2 Gene in domestic cats between 2006–2008 and 2012–2014, Portugal. *Transboundary and emerging diseases* 64: 1178–1183. <https://doi.org/10.1111/tbed.12483>.
- Ndiana, L.A., G. Lanave, A.A.K. Zarea, C. Desario, E.A. Odigie, F.A. Ehab, P. Capozza, G. Greco, C. Buonavoglia, and N. Decaro. 2022. Molecular characterization of carnivore protoparvovirus 1 circulating in domestic carnivores in Egypt. *Frontiers in veterinary science* 9: 932247. <https://doi.org/10.3389/fvets.2022.932247>.
- Parker, J.S., and C.R. Parrish. 1997. Canine parvovirus host range is determined by the specific conformation of an additional region of the capsid. *Journal of virology* 71: 9214–9222. <https://doi.org/10.1128/JVI.71.12.9214-9222.1997>.
- Parker, J.S., W.J. Murphy, D. Wang, S.J. O'Brien, and C.R. Parrish. 2001. Canine and feline parvoviruses can use human or feline transferrin receptors to bind, enter, and infect cells. *Journal of virology* 75: 3896–3902. <https://doi.org/10.1128/JVI.75.8.3896-3902.2001>.
- Parrish, C.R. 1991. Mapping specific functions in the capsid structure of canine parvovirus and feline panleukopenia virus using infectious plasmid clones. *Virology* 183: 195–205. [https://doi.org/10.1016/0042-6822\(91\)90132-u](https://doi.org/10.1016/0042-6822(91)90132-u).
- Truyen, U., and C.R. Parrish. 1992. Canine and feline host ranges of canine parvovirus and feline panleukopenia virus: distinct host cell tropisms of each virus in vitro and in vivo. *Journal of virology* 66: 5399–5408. <https://doi.org/10.1128/jvi.66.9.5399-5408.1992>.
- Truyen, U., M. Agbandje, and C.R. Parrish. 1994. Characterization of the feline host range and a specific epitope of feline panleukopenia virus. *Virology* 200: 494–503. <https://doi.org/10.1006/viro.1994.1212>.
- Truyen, U., A. Gruenberg, S.F. Chang, B. Obermaier, P. Veijalainen, and C.R. Parrish. 1995. Evolution of the feline-subgroup parvoviruses and the control of canine host range in vivo. *Journal of virology* 69: 4702–4710. <https://doi.org/10.1128/JVI.69.8.4702-4710.1995>.
- Wang, J., X. Chen, Y. Zhou, H. Yue, N. Zhou, H. Gong, and C. Tang. 2022. Prevalence and characteristics of a feline parvovirus-like virus in dogs in China. *Veterinary microbiology* 270: 109473. <https://doi.org/10.1016/j.vetmic.2022.109473>.
- Wen, F.T., S.M. Bell, T. Bedford, and S. Cobey. 2018. Estimating vaccine-driven selection in seasonal influenza. *Viruses* 10 (9): 509. <https://doi.org/10.3390/v10090509>.
- Xue, H., C. Hu, H. Ma, Y. Song, K. Zhu, J. Fu, B. Mu, and X. Gao. 2023. Isolation of feline panleukopenia virus from Yanji of China and molecular epidemiology from 2021 to 2022. *Journal of veterinary science* 24: e29. <https://doi.org/10.4142/jvs.22197>.
- Yang, Y., Zheng, M., Liu, Y., Wang, Y., Xu, Y., Zhou, Y., Sun, D., Chen, L., Li, H., 2021. Analysis of Intermediate Hosts and Susceptible Animals of SARS-CoV-2 by Computational Methods. *Zoonoses* 1. <https://doi.org/10.15212/ZOONOSES-2021-0010>.
- Yi, S., S. Liu, X. Meng, P. Huang, Z. Cao, H. Jin, J. Wang, G. Hu, J. Lan, D. Zhang, Y. Gao, H. Wang, N. Li, N. Feng, R. Hou, S. Yang, and X. Xia. 2021. Feline panleukopenia virus with G299E substitution in the VP2 protein first identified from a captive Giant Panda in China. *Frontiers in cellular and infection microbiology* 11: 820144. <https://doi.org/10.3389/fcimb.2021.820144>.
- Yuan, K., D. Wang, Q. Luan, J. Sun, Q. Gao, Z. Jiang, S. Wang, Y. Han, X. Qu, Y. Cui, S. Qiu, Y. Di, X. Wang, S. Song, P. Wang, S. Xia, Y. Yu, W. Liu, and Y. Yin. 2020. Whole genome characterization and genetic evolution analysis of a new ostrich parvovirus. *Viruses* 12 (3): 334. <https://doi.org/10.3390/v12030334>.

Publisher's Note

Springer Nature remains neutral with regard to jurisdictional claims in published maps and institutional affiliations.